RSC Advances

ROYAL SOCIETY OF CHEMISTRY

www.rsc.org/advances

Graphical abstract

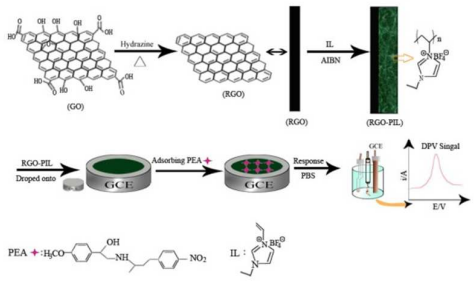

The preparation for a novel composite of RGO-PIL and its electrochemical sensor for sensitive detecting phenylethanolamine A.

Cite this: DOI: 10.1039/c0xx00000x

www.rsc.org/xxxxxx

ARTICLE TYPE

Electrochemical sensor for sensitive determination of phenylethanolamine A based on a novel composite of reduced graphene oxide and poly(ionic liquid)

Jinchun Li,[a] Qian Li,[ab] Yanbo Zeng,*[b] Ting Tang,[b] Yangdan Pan,[b] and Lei Li*[ab]

Received (in XXX, XXX) Xth XXXXXXXXX 20XX, Accepted Xth XXXXXXXXX 20XX
DOI: 10.1039/b000000x

In this paper, we reported an electrochemical sensor for phenylethanolamine A (PEA) that was based on a novel composite of reduced graphene oxide and poly(ionic liquid) (RGO-PIL). The RGO-PIL composite was prepared by radical polymerization of 1-vinyl-3-ethylimidazolium tetrafluoroborate monomer on graphene matrix. The RGO-PIL composite was characterized by Fourier transform infrared spectroscopy, thermal gravimetric analysis, scanning electron microscopy, Raman spectroscopy and X-ray diffraction. The RGO-PIL sensor involved the advantages, such as good electrocatalytic property and large surface area. Due to the synergistic contribution of RGO and PIL, the RGO-PIL sensor can be applied for detecting PEA with high sensitivity. In addition, compared with PIL sensor and bare electrode, the RGO-PIL sensor had highest peak current response. Under the optimal experiment conditions, the reduction peak current was proportional to the concentration of PEA from 0.005 to 10.0 μM with the detection limit of 0.002 μM. Owing to the electrochemical reduction of the nitro group for PEA, 1000-fold of clenbuterol, ractopamine, and salbutamol did not interfere with PEA determination based on RGO-PIL sensor. The RGO-PIL sensor not only exhibited good stability with adequate reproducibility and accuracy, but also demonstrated efficiency in the determination of PEA for pig urine samples.

Introduction

Graphene, a two-dimensional monolayer of carbon atoms arranged in honeycomb lattice, has received tremendous attention from both the experimental and the theoretical scientific communities.[1,2] In recent years, unique electronic properties, mechanical properties and extremely large surface area endow graphene and graphene-based composites with more applications. Among them, ionic liquid/graphene,[3] Cu_2O/graphene,[4] Ag-Au/graphene,[5] $NiFe_2O_4$/graphene,[6] and etc.[7] have been prepared for electrode modifiers in electrochemical sensors based on their good electrocatalytic activity and large surface area. In addition, graphene could serve as the reinforcing element in a polymer matrix in fabricating new advanced materials. This combination between graphene and polymer offers an attractive route to introduce some novel properties.[8,9] Some groups have already functionalized graphene with various polymers to assemble the composites with desired properties. The efforts were mainly made on the effective dispersibility of the composites,[10] adsorption for target molecules,[11,12] and improvement of the electrical conductivity,[13,14] and mechanical strength of the composites.[15]

Polymeric ionic liquids (PILs) are polymeric analogues of ionic liquids, which are obtained via polymerization of ionic liquid monomers.[16] Being a novel polymeric material, PILs exhibit the advantages of both ionic liquids and polymers, such as enhanced ionic conductivity, thermal stability and excellent mechanical properties. PILs have broaden the properties and applications of room temperature ionic liquids.[17,18] Being novel polymeric materials, PILs have been proved to be effective stabilizers or supporters for the synthesis and functionalization of various nanomaterials, such as carbon nanotubes,[19,20] ordered mesoporous carbons,[21] magnetic nanoparticles,[22] noble metal nanoparticles[23,24] and graphene.[25,26] For example, PIL-graphene based on 1-vinyl-3-ethylimidazolium bis (trifluoromethylsulfonyl) amide was prepared for a supporter of Ag nanoparticles, which was used for electrochemical sensing hydrogen peroxide.[25] PIL-graphene composite based on 1-vinyl-3-butylimidazolium bromide was a good supporter for enzyme immobilization and the biosensor exhibited superior performance for glucose.[26] However, there is still much work to study the more application of PILs through synthesizing new PIL-functionalized graphene composites and fabricate electrochemical sensors based on these composites. To the best of our knowledge, the composite of graphene and poly(ionic liquid) based on the ionic liquid of 1-vinyl-3-ethylimidazolium tetrafluoroborate ([VEIM]BF_4) has not been reported.

β-Agonists were originally used as therapeutic treatments for asthma and preterm labour in humans.[27] These drugs have also been misused as nutrient repartitioning agents in livestock, where they served to divert nutrients from fat deposition in animals to the production of muscle tissues.[28] However, these drugs may remain in animal derived food and consumption of contaminated meat products may pose potential risks to adverse cardiovascular and central nervous system effects.[29] Therefore, β-agonists are banned as feed additives of animals for growth promotion in many countries. The most commonly abused β-adrenergic

agonists are clenbuterol, salbutamol and ractopamine. Unfortunately, with the crackdown of banned β-agonists, some other new β-agonists were emerged. A new alternative of β-adrenergic agonist named phenylethanolamine A (PEA) has been illegally used in livestock in China. Phenylethanolamine A is a phenethanolamine member of the family of β-agonists. It is a synthetic substance and the isomer of formoterol, and structurally similar to ractopamine (See Figure 1).[30] Since 2010, PEA has been prohibited from being used in feeds and animal drinking water in bulletin no. 1519 issued by the Ministry of Agriculture of China. So it is necessary to develop a sensitive, effective and simple method for determination of PEA in actual samples.

Many analytical techniques, including high performance liquid chromatography-tandem mass spectrometry[31] and enzyme-linked immunosorbent assay,[30,32] have been used to develop sensitive, convenient and effective methods for PEA residue analysis. Although chromatographic methods are accurate, they are expensive and time-consuming. The enzyme-linked immunosorbent assays (ELISAs) have some advantages, such as high specificity and throughput. However, ELISAs require the complicated synthesis of immunogen for PEA. Therefore, there is an urgent need to develop low-cost, sensitive and specific analytical method for the detection of PEA in tissue and feed samples. Electrochemical method possesses high sensitivity, good selectivity and low-cost instrumentation. It is fit to analyze PEA concentration in actual samples. Few papers reported PEA determination with electrochemical method up to now.

The aim of this work is to fabricate a novel and stable electrochemical sensor for sensitive determination of PEA. The working electrode used in this method was modified with RGO-PIL composite. The RGO-PIL composite was prepared by radical polymerization of 1-vinyl-3-ethylimidazolium tetrafluoroborate monomer on graphene matrix. The RGO-PIL sensor involved the advantages, such as good electrocatalytic property and large surface area of RGO and PIL. Due to the synergistic contribution of RGO and PIL, RGO-PIL sensor can be applied for detecting PEA with high sensitivity. The experimental parameters including RGO-PIL concentration, adsorption time and pH value were optimized. Finally, this method was successfully applied to detect PEA in pig urine samples with satisfactory results.

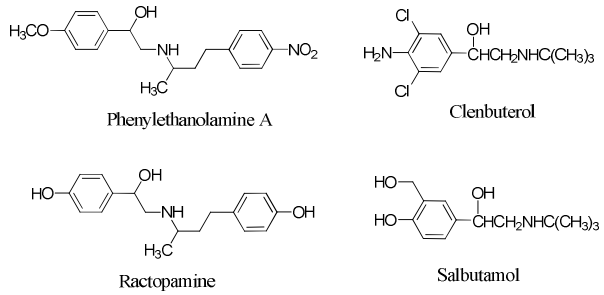

Figure 1. Chemical structures of PEA and some related compounds.

Experimental Section

Reagents and Materials

Graphite (spectral grade), 2,2-azobisisobutyronitrile (AIBN) were purchased from Shanghai Sinopharm Chemical Reagent Co., Ltd. 1-vinyl-3-ethylimidazolium tetrafluoroborate ([VEIM]BF_4) was purchased from Lanzhou Institute of Chemical Physics. Phenylethanolamine A (PEA) was purchased from Witega Laboratorien Berlin-Adlershof GmbH (Germany). Ractopamine (RAC) was purchased from Dr. Ehrenstorfer GmbH (Germany). Clenbuterol (CLB) and salbutamol (SAL) were purchased from the National Institutes for Food and Drug Control (China). Other chemicals were of analytical grade and were purchased from Aladdin Industrial Corporation (Shanghai, China). Phosphate buffer solution (PBS, 0.05 mol/L) with different pH was prepared by mixing the stock solutions of KH_2PO_4 and Na_2HPO_4, with 0.5 mol/L NaCl added as the supporting electrolyte. The twice deionized water was used throughout the experiments.

Equipment and Characterizations

Surface morphological images were recorded by a Hitachi S-4800 scanning electronic microscope (SEM) (Hitachi, Japan). Fourier transform infrared (FTIR) spectroscopic measurements were performed on Agilent 640 Fourier transform infrared spectrometer (Agilent, USA). Thermal gravimetric analysis (TGA) was conducted on a STA-409PC instrument from room temperature to 800 °C with a heating rate of 10 °C min^{-1} in the nitrogen flow (Netzsch, German). Raman measurements were carried out using a in Via-Reflex Raman spectroscope equipped with a 532 nm laser source (Renishaw, England). X-ray diffraction (XRD) patterns were recorded by by a DX-2600 X-ray diffractometer (Dandong, China), which was operated at 30 kV and 20 mA at a scan rate of 0.05°/s using Cu Kα radiation (λ=0.1542 nm).

All electrochemical experiments were performed on a CHI 660D electrochemical workstation (CHI Instruments Co., Shanghai, China) with a conventional three electrode system comprising platinum wire as auxiliary electrode, an Ag/AgCl electrode as reference electrode and the modified or unmodified glass carbon electrode (3 mm diameter, GCE) as working electrode.

Synthesis of RGO-PIL

GO was prepared using a modification of Hummers and Offeman method from graphite powders.[33,34] RGO was synthesized by incomplete reduction of GO. Briefly, 0.1 g of GO was added to 200 mL of water, followed by sonicating for 2 h. Then, 0.1 mL of ammonia (28% w/w) and 1.4 mL of hydrazine (80% w/w) were added to the GO resultant dispersion. After being vigorously stirred for a few minutes, the reaction mixture was stirred for 1 h at 95 °C. After this, the mixture turned its color from brown to black, which indicated the reduction of GO to RGO.

0.02 g of RGO was dispersed in 20 mL of methanol. After ultrasonication for 30 min, 0.1 g of [VEIM]BF_4 and 50 mg of AIBN was added to the mixture. The resulting solution was stirred with nitrogen for 15 min. The temperature was increased

to 70 °C, and the reaction was allowed to proceed for 12 h. The resulting product was collected and washed with twice deionized water, ethanol. At last the obtained product was dried over night in a vacuum oven to obtain RGO-PIL.

Electrochemical measurements

The GCE was polished with 0.05 mm alumina slurry, followed by rinsing with twice deionized water, and then treated by ultrasonication in nitric acid (1:1, v/v), 1 M NaOH, acetone, and twice-distilled water. 5 mg of RGO-PIL (or PIL) was dispersed in 1 mL of N,N-dimethylformamide with ultrasonication for 30 min. 5 μL of the above suspensions were dropped on the clean GCE surface and dried under an infrared lamp. PBS (0.05 mol/L, pH=5.0) with 0.5 mol/L NaCl added as the supporting electrolyte. The electrolyte solution was purged with nitrogen for 10 min and maintained under nitrogen atmosphere during the measurements. The modified electrodes were incubated in 5 mL of PEA solution for 5 min and measured by differential pulse voltammetry (DPV) in PBS. Then, differential pulse voltammograms of the modified electrode which had adsorbed PEA were recorded between -0.2 and -1.0 V. The pulse amplitude, pulse period, and pulse width of DPV were 50 mV, 0.2 s, and 50 ms, respectively.

Sample collection and pretreatment

Pig urine samples were provided by Jiaxing Bureau of Quality and Technical Supervision. Prior to analysis, the samples were centrifuged for 10 min at 8000 r/min in order to remove precipitated proteins and other particulate matters.

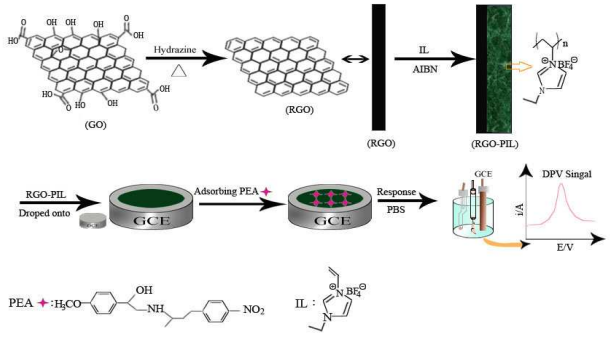

Figure 2. Illustration of the preparation for RGO-PIL and electrochemical detecting PEA of its sensor.

Results and Discussion

Preparation and characterization of RGO-PIL

Figure 2 presented illustration of the preparation procedure for RGO-PIL and detection process for its electrochemical sensor. Details of the preparation could be found in the experimental section. First, RGO was synthesized from the incomplete reduction of GO. Then RGO-PIL was successfully obtained by the copolymerization in presence of RGO, [VEIM]BF_4. RGO-PIL was used as a electrode material in the construction of an electrochemical sensor for PEA.

Characterization of GO, RGO, RGO-PIL

Figure 3A showed the FTIR spectra of GO, RGO and RGO-PIL. GO exhibited one characteristic peak at about 3426 cm^{-1} (curve a), which corresponded to the O-H stretching vibration. A sharp peak at 1722 cm^{-1} was attributed to C=O stretch vibration. After the reduction, the peak intensity of 3426 cm^{-1} for O-H group decreased significantly and the peak of 1722 cm^{-1} disappeared. However, some peaks can be seen from curve b, for example, the peak at about 1395 cm^{-1} arised from O-H deformation stretching vibration of the C-OH group. The peak at 1634 cm^{-1} was due to the C=C groups, which directed the selective polymerization on the RGO surface.[35] As shown from curve c, RGO-PIL showed the characteristic peaks at 1559 cm^{-1} and 1168 cm^{-1}, which were attributed to the C=N and C-N stretching vibration of imidazole functional groups of PIL. All these peaks confirmed the successful synthesis of RGO-PIL.

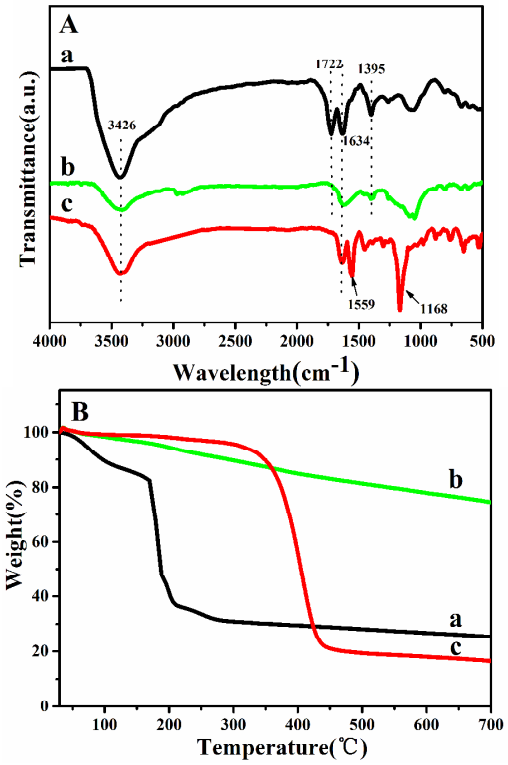

Figure 3. (A) FTIR spectra of GO (a), RGO (b) and RGO-PIL(c); (B) TGA curves of GO (a), RGO (b) and RGO-PIL (c).

The thermal stability of GO, RGO and RGO-PIL was investigated by TGA. Figure 3B showed that GO was unstable at an elevated temperature and about 17.5% weight loss occurs at 170 °C (curve a). This was ascribed to the loss of residual water between the adjacent hydrophilic GO sheets. A sharper weight loss near 200 °C was also observed, which was due to the pyrolysis of oxygen-containing groups from the surface of GO. And GO had about 75% total weight loss within 700 °C. In comparison to GO, RGO showed a more gradual and smaller weight loss (curve b), indicating that the thermal stability of RGO was improved after the reduction. In addition, RGO had about 25% total weight loss, which was attributed to some oxygen groups on RGO surface. This suggested that RGO was prepared

through incomplete reduction of GO. The TGA curve of RGO-PIL (curve c) showed a gradual weight loss below 300 °C, which was likely due to the decomposition of labile oxygen functional groups. The weight of RGO-PIL declined sharply between 300 °C and 450 °C, which might be attributed to the skeleton degradation for PIL. And RGO-PIL became stable above 450 °C with about 83% total weight loss, which can be ascribed to the thermal instability of PIL. The different thermal stability between RGO and RGO-PIL revealed that PIL was successfully grafted on the RGO surface.

The surface morphology of GO, RGO and RGO-PIL were investigated by SEM. As shown in Figure 4A, GO displayed layered structures with sheets crumpled or wrinkled. Compared with GO, RGO exhibited more wrinkled layers in quantity (Figure 4B). The SEM image of RGO-PIL in Figure 4C revealed thicker wrinkled layers compared with RGO, indicating PIL had been grafted to RGO.

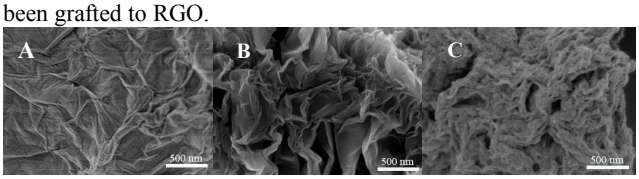

Figure 4. SEM images of GO (A), RGO (B) and RGO-PIL(C).

Raman spectroscopy is also a powerful way to characterize carbon materials. Figure 5A was the Raman spectra of GO, RGO and RGO-PIL. We could see two intensive peaks at about 1343 cm^{-1} and 1589 cm^{-1}. These two strong peaks were attributed to D band and G band,[36] which refer to the D band, resulting from a disordered sp^3 carbon structure, and the G band representing sp^2 ordered crystalline graphite-like structures, respectively. For our samples, the I_D/I_G ratios of the GO, RGO and RGO-PIL were 0.78, 1.05 and 1.07, respectively. In general, the increase of I_D/I_G ratio reflected the increasing disorder present within in materials.[37] The initial GO showed a minimal disorder mode, and the I_D/I_G ratio of RGO-PIL had a great increase, which can be also attributed to the covalent interaction between PIL and RGO.[38] Besides, it can be observed that the peak intensities of RGO-PIL were weaker than that of RGO under the same characterization conditions. The phenomenon originated from the lower content of RGO in the RGO-PIL composite, indicating PIL had been successfully grafted to RGO.

The XRD patterns of GO, RGO and RGO-PIL were shown in Figure 5B. Similar to the previous report,[39] GO and RGO showed a XRD peak at 2θ=10.5° (curve a) and 2θ=24.5° (curve b), indicating an interlayer spacing of 0.843 nm and 0.363 nm. The decreased interlayer spacing for RGO was due to the removal of oxygen-based functional groups on the basal plane by thermal reduction. Compared with RGO, the diffraction peak of RGO-PIL shifted to 2θ=22.65° (curve c), indicating the interlayer spacing of 0.393 nm. This could be explained by the slight broadening of interlayer spacing due to the effect of PIL.[40] The result revealed that PIL was successfully grafted onto the RGO surface.

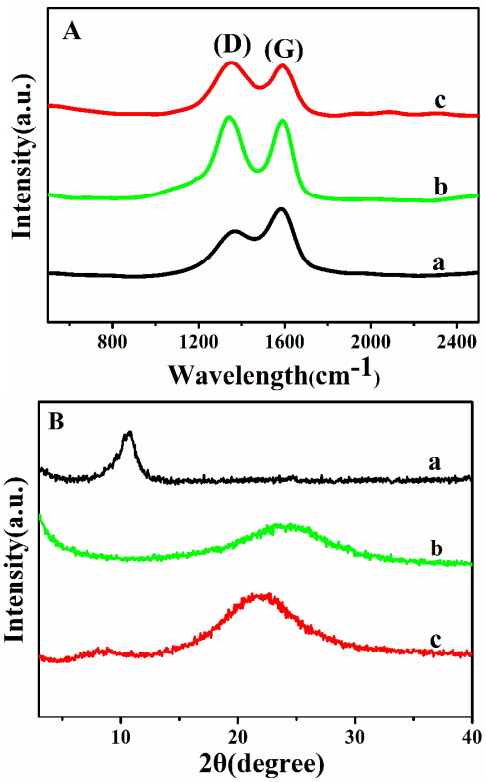

Figure 5. (A) Raman spectra of GO (a), RGO (b) and RGO-PIL (c); (B) XRD patterns of GO (a), RGO (b) and RGO-PIL (c).

Electrochemical behavior of the modified electrodes

Cyclic voltammetry was used to study the electrochemical properties of materials. The CVs of the electrochemical sensor were investigated in 5.0 mmol/L $K_3[Fe(CN)_6]$ solution containing 0.1 mol/L KCl as shown in Figure 6. the bare GCE showed a reversible redox reaction with a peak potential difference of 95 mV and a peak current ratio of about 1:1 (curve c). When the electrode surface was covered with the PIL, the redox peak current was increased (curve b), indicating the incorporation of PIL improved the current response of $K_3[Fe(CN)_6]$ on the PIL/GCE. When the electrode was coated with RGO-PIL, larger redox peak was observed at RGO-PIL/GCE compared to bare GCE or PIL/GCE (curve a). The increment of peak current may be attributed the synergistic contribution of RGO and PIL with good conductivity, which could promote the redox reaction of $[Fe(CN)_6]^{3-/4-}$ on the electrode surface.

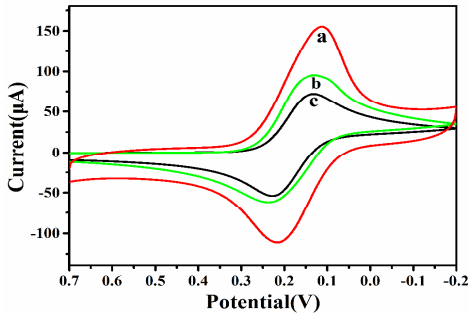

Figure 6. Cyclic voltammograms of 5 mM $K_3[Fe(CN)_6]$ in 0.1 M KCl solution at RGO-PIL/GCE (a), PIL/GCE (b) and bare GCE (c).

Electrochemical effective surface area

As shown in Figure 7A and B, the electrochemical effective surface area for RGO-PIL/GCE, PIL/GCE and GCE can be calculated by the slope of the plot of Q vs. $t^{1/2}$, which was obtained by chronocoulometry using 0.5 mM $K_3[Fe(CN)_6]$ as model complex based on Eq. (1) given by Anson:[41]

$$Q(t) = \frac{2nFACD^{1/2}t^{1/2}}{\pi^{1/2}} + Q_{dl} + Q_{ads} \quad (1)$$

where n is the number of transfer electron (n of $K_3[Fe(CN)_6]$ is 1), A is the surface area of the working electrode, C is the concentration of substrate, D is the diffusion coefficient (D of $K_3[Fe(CN)_6]$ is 7.6×10^{-6} cm^2 s^{-1}), Q_{dl} is double layer charge which could be eliminated by background subtraction, Q_{ads} is Faradic charge. As shown in Figure 7B, the slope of the linear relationship between Q and $t^{1/2}$ for RGO-PIL/GCE, PIL/GCE and bare GCE can be obtained to be 3.98×10^{-5}, 1.29×10^{-5} and 6.24×10^{-6}, respectively. Thus A can be calculated as 0.265, 0.086 and 0.042 cm^2, correspondingly. The results indicated that the electrochemical effective surface area was increased obviously after modification of GCE with RGO-PIL, which could enhance the total adsorption capacity of PEA,[42] leading to the increase of current response of PEA.

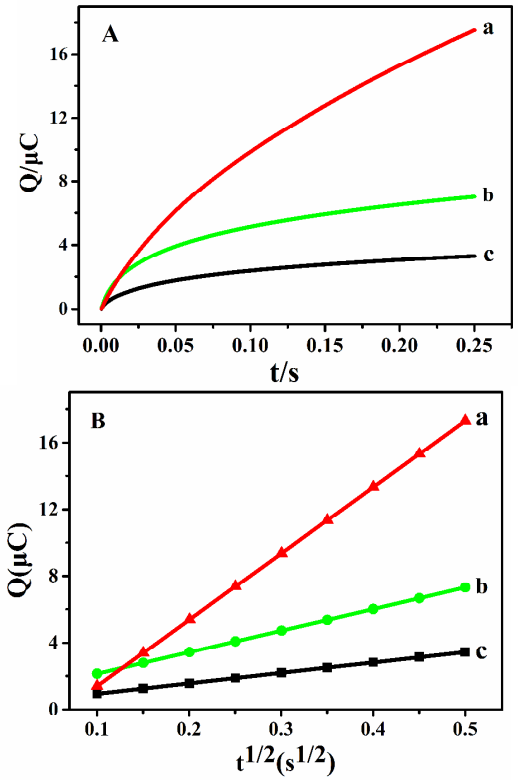

Figure 7. (A) Plot of Q–t curves for the RGO-PIL/GCE (a), PIL/GCE (b) and GCE (c) in 0.5 mM $K_3[Fe(CN)_6]$; (B) Plot of Q–$t^{1/2}$ curves for the RGO-PIL/GCE (a), PIL/GCE (b) and GCE (c) in 0.5 mM $K_3[Fe(CN)_6]$. The pulse width, sample interval and quiet time of chronocoulometry were 0.25 s, 0.25 ms, and 2 s, respectively.

Electrochemical sensing of PEA

The cyclic voltammograms of RGO-PIL/GCE in the absence (curve a) and presence (curve b and curve c) of 10.0 μM PEA were shown in Figure 8A. No redox peak could be observed in PBS blank solution (curve a). However, PEA exhibited well-defined voltammetric peaks, which were observed at the RGO-PIL/GCE in presence of 10.0 μM PEA. In the first cycle (curve b), a irreversible reduction peak (Epc1, -0.522V) could be observed, which corresponded to the reduction of the nitro group to hydroxylamine group via a four-electron process (reaction 1, Figure 8C).[43] Then it was oxidized to the nitroso group (Epa, 0.103 V, reaction 2). In the following second cycle (curve c), the appearance of another reduction peak (Epc2, 0.026 V, reaction 3) was ascribed to reverse process of reaction 2. The pair of reversible redox peaks should be attributed to a two-electron transfer redox process. The peak Pc1 dropped dramatically in the second cycle, which should be due to the reaction exhaustion of PEA at the surface of RGO-PIL/GCE.

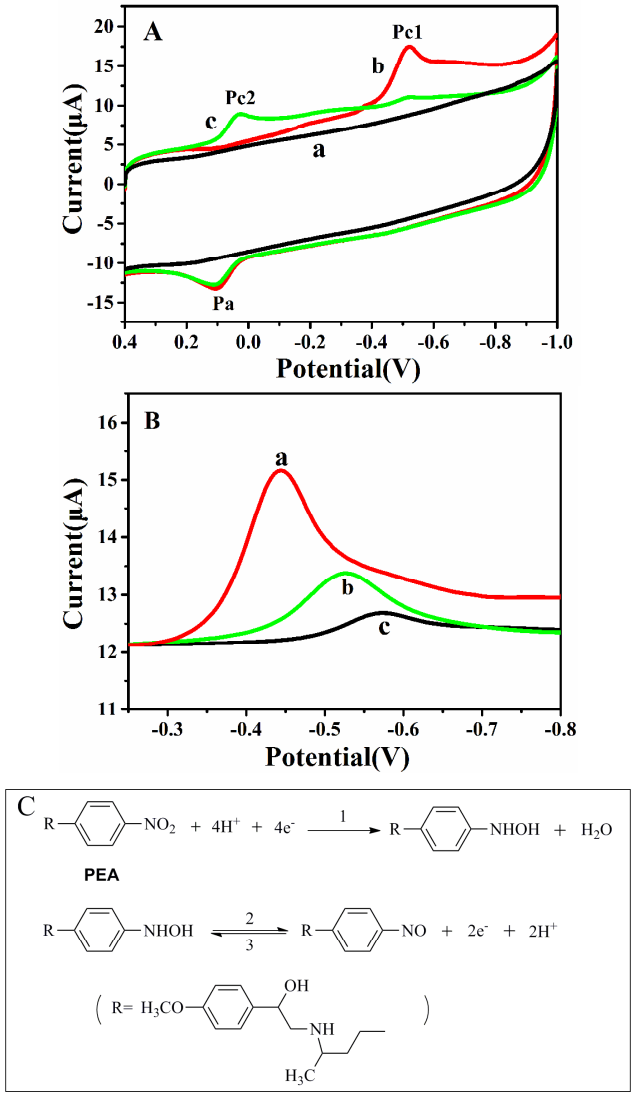

Figure 8. (A) Cyclic voltammograms of RGO-PIL/GCE in the absence (a) and presence (b: the first cycle and c: the second cycle) of 10 μM PEA; (B) Differential pulse voltammograms of RGO-PIL/GCE (a), PIL/GCE (b) and GCE (c) in the presence of 5 μM PEA. Supporting electrolyte: 0.05 mol/L PBS (pH 5.0, 0.5 mol/L NaCl), scan rate: 100 mv/s, adsorption time: 5 min; (C) Mechanism of the electrochemical reaction of PEA at RGO-PIL/GCE.

As shown in Figure 8B, differential pulse voltammograms of RGO-PIL/GCE (curve a), PIL/GCE (curve b) and bare GCE (curve c) in the presence of 5.0 μM PEA were measured from -0.2 to -0.8 V. There were obvious DPV peaks observed at these electrodes, which should be attributed to the irreversible reduction of the nitro group to hydroxylamine group. Among these electrodes, the lowest current response for PEA was observed at bare GCE, which had the potential of reductive peak at -0.568 V. When the GCE was modified with PIL, the reduction current increased and the peak potential positively shifted to -0.528 V, suggesting that PIL had effective catalytic ability to reduce PEA.[25,44] When the GCE was modified with RGO-PIL, the highest current response was observed and the peak potential positively shifted to -0.448 V, which was also due to good electrocatalytic property of RGO-PIL.

Optimization of experimental conditions

RGO-PIL which was dropped on the electrode surface played an important role in PEA reduction. In our experiment, the response concentration of PEA was 5.0 μM, and the volume of the different suspensions dropped onto the GCE surface was controlled to be 5.0 μL. With increasing RGO-PIL concentration from 1.0 to 5.0 mg mL^{-1}, the DPV peak current at RGO-PIL/GCE increased obviously (Figure 9A). It might ascribe to the expansion of conductive electrode area and the increase of accumulation ability. Further the increase of the RGO-PIL concentration led to a decrease in the peak current. It was probably due to the fact that a thicker RGO-PIL film hampered the transfer of PEA molecules to GCE surface. Hence, a concentration of 5.0 mg mL^{-1} RGO-PIL was chosen to modify GCE for electrochemical detection of PEA.

As shown in Figure 9B, the response time of RGO-PIL/GCE for 5.0 μM PEA was investigated by varying the adsorption time from 1 min to 8 min. A response equilibrium of 63.2% was achieved within a period of 3 min and the response equilibrium reached within 5 min. The result revealed rapid response equilibrium of PEA molecules to RGO-PIL.

The effect of pH on the electrochemical response for 5.0 μM PEA at RGO-PIL/GCE was studied over the pH ranging from 3.5 to 6.5 (Figure 9C). The reduction current increased gradually over the pH range from 3.5 to 5.0. While the pH value exceeded 5.0, the reduction current decreased. Therefore, 5.0 of pH value was selected as the supporting electrolyte.

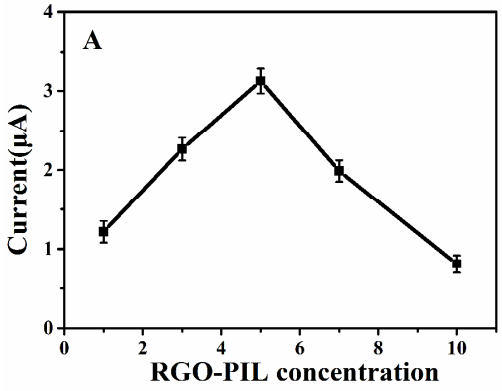

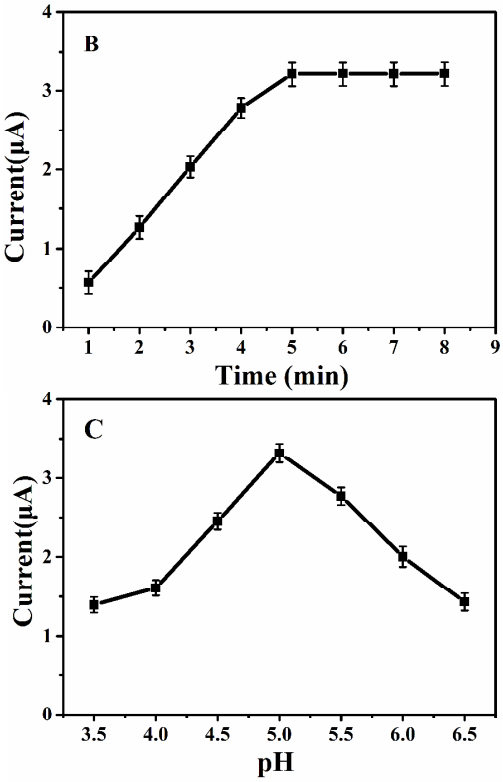

Figure 9. The effect of RGO-PIL concentration (A), adsorption time (B) and pH (C) on DPV peak current response of RGO-PIL/GCE for 5 μM PEA.

Linearity, reproducibility and stability of RGO-PIL sensor

Under the optimal experiment conditions, DPV was used to investigate the linearity and detection limit of RGO-PIL sensor (RGO-PIL/GCE) for PEA. As shown in Figure 10A and B, the current responses increased with successive addition of different PEA concentrations in PBS. Figure 10C illustrated the corresponding plot showing a linear relation between current response and PEA concentration in the range of 0.005 to 10.0 μM, The regression equation was: I(μA)=0.582(μM)+0.439 (R=0.9986).

To obtain the limit of detection (LOD), we used an IUPAC-recommended methodology that utilizes an experimentally determined signal-to-noise ratio (S/N).[45,46] We measured 11 replicate detections of the blank solution, based on this, an average current for blank ($average_{blank}$) along with the associated standard deviation (SD_{blank}) was determined. This SD_{blank} was regarded as the noise (N) of our detection system. Next, detection was performed from samples with a known, relatively low concentration of target sequences. The resultant current at the same concentration was measured five times, and the average value ($average_{sample}$) was calculated. Finally, S/N was calculated as follows:

$$S/N = (average_{sample} - average_{blank})/SD_{blank}$$

If the S/N was greater than 5, the sample was diluted to half the initial concentration and the S/N determination was repeated until the S/N value fell within the range of 3 to 5. A sample concentration that meeted the condition of $3 < S/N < 5$ was determined as the LOD of our detection platform. In our experiment, the SD_{blank} of blank solution was 3.1%. The average currents of 0.001 μM, 0.002 μM, 0.003 μM PEA were 0.1070 μA, 0.1527 μA, 0.2158 μA (Insets of Figure 10C), respectively. The signal-to-noise ratios were caulated as 2.00, 3.47, 5.51,

respectively. Thus the LOD of RGO-PIL sensor for PEA determination was 0.002 μM. As shown in Table 1, the results of RGO-PIL sensor were compared with that of other published methods detecting β-agonists.[47-53] The results demonstrated wide linear range and low LOD of the prepared RGO-PIL sensor for PEA.

Table 1 The comparison with other electrochemical methods for the determination of β-agonists.

Electrochemical sensing platform	Detection method	Analyte	Linear range (μM)	LOD (μM)	Ref.
Nafion/MWCNTs/AuNPs /GCE	LSV[a]	PEA	0.01-10.0	0.005	47
MIP/ISE[b]	potential	Clenbuterol	0.1-100.0	0.07	48
Nafion-Au/GCE	DPV	Clenbuterol	0.8-10.0	0.1	49
Au/L-cys/MWNTs-NF[c]/GCE	LSV	Salbutamol	0.09-7.0	0.05	50
DNA/PAn-LB[d]/GCE	DPV	Salbutamol	0.1-10.0	0.08	51
MWCNT-MIP/SPE[e]	DPV	Ractopamine	0.02-0.2	0.006	52
OMC[f]/GCE	DPV	Ractopamine	0.085-8.0	0.06	53
RGO-PIL/GCE	DPV	PEA	0.005-10.0	0.002	This work

LSV[a] : linear sweep voltammetry;
ISE[b]: ion selective electrode;
L-cys/MWNTs-NF[c]: L-cysteine/ MWNTs-Nafion;
PAn-LB[d]: polyaniline-Langmuir-Blodgett;
SPE[e]: screen-printed electrode;
OMC[f]: ordered mesoporous carbon.

So as to confirm the advantages of RGO-PIL sensor, we investigated the linearity of PIL and bare GCE sensors (Figure 10C). The regression equations were: I(μA)=0.189C(μM)+0.383 (R=0.9945) (PIL sensor) and I(μA)=0.0456C(μM)+0.149 (R=0.9959) (bare GCE), respectively. $K_{RGO-PIL}$, K_{PIL} and K_{GCE} were the linear slopes of RGO-PIL, PIL sensors and bare GCE. So $K_{RGO-PIL}$, K_{PIL} and K_{GCE} were 0.582, 0.189 and 0.0456, respectively. The ratios of $K_{RGO-PIL}/K_{PIL}$, $K_{RGO-PIL}/K_{GCE}$ and K_{PIL}/K_{GCE} were 3.08, 12.76 and 4.14, respectively, indicating RGO-PIL sensor exhibited higher current response, which could be attributed to the synergistic effect of good electrocatalytic property and large surface area for RGO-PIL composite.

The reproducibility of RGO-PIL sensor was also evaluated by using the same electrode for 8 repeated analyses of 3.0 μM PEA, with a relative standard deviation (RSD) of 4.8%. Moreover, the sensor retained a response of 92.6% of the initial current after storage for two weeks in room temperature. The results showed that this sensor had a good reproducibility and stability.

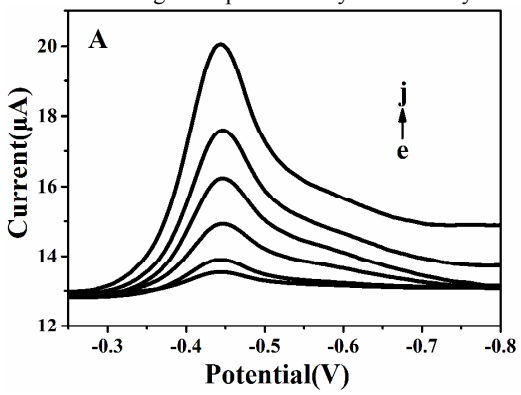

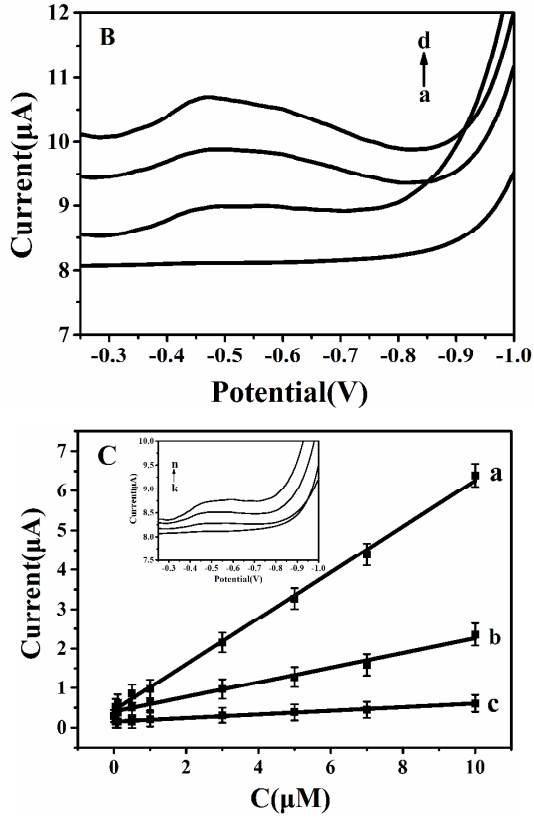

Figure 10. (A) Differential pulse voltammograms of RGO-PIL sensor for PEA, PEA concentration (e-j): 0.5, 1.0, 3.0, 5.0, 7.0, 10.0 μM; (B) Differential pulse voltammograms of RGO-PIL sensor for PEA, PEA concentration (a-d): 0, 0.005, 0.05, 0.1 μM; (C) Calibration curves of PEA detection obtained by RGO-PIL (a), PIL sensors (b) and bare GCE (c) (n=3), insets: differential pulse voltammograms of RGO-PIL sensor for PEA, PEA concentration (k-n): 0, 0.001, 0.002, 0.003 μM. Supporting electrolyte: 0.05 mol/L PBS (pH 5.0, 0.5 mol/L NaCl), adsorption time: 5 min.

Interference studies

In order to apply the proposed method in urine samples, it is vital to investigate the effect of potential interference substances on PEA determination, which was used to evaluate the selectivity of RGO-PIL sensor for PEA. Potential interference substances involved some ions, β-agonists, amino acids and sugars. The DPV determination of 5.0 μM PEA was tested in presence of spiked known amounts of interfering substances. The tolerance limit was defined as the amount and fold of the interfering substances causing a change of ±5% in the peak current intensity reading. The tolerable limits of interfering substances were given in Table 2. The results showed that 1000-fold of Na^+, K^+, Mg^{2+}, Cl^-, NO_3^-, SO_4^{2-}, CO_3^{2-}, PO_4^{3-}, L-serine, β-alanine, L-threonine, L-histidine, and L-cysteine, did not interfere with PEA determination. In addition, 500-fold of starch, maltose, glucose, sucrose, ascorbic acid, uric acid, and urea also did not interfere the determination of PEA. Specifically, 1000-fold of other β-agonists including clenbuterol, ractopamine, and salbutamol did not interfere with PEA determination, which was attributed to the electrochemical reduction of the nitro group for PEA. The results indicated that the RGO-PIL sensor exhibited good selectivity.

Table 2 The tolerance limit of interfering substances on the determination of 5.0 μM PEA using RGO-PIL sensor.

Interfering substances	Tolerance limit (μM, fold)
Na^+, K^+, Mg^{2+}, Cl^-, NO_3^-, SO_4^{2-}, CO_3^{2-}, PO_4^{3-}	5.0×10^3, 1000
Clenbuterol, ractopamine, salbutamol	5.0×10^3, 1000
Starch, maltose, glucose, sucrose	2.5×10^3, 500
L-Serine, β-alanine, L-threonine, histidine, L-cysteine	5.0×10^3, 1000
Ascorbic acid, uric acid, urea	2.5×10^3, 500

Analytical application

To demonstrate the feasibility of RGO-PIL sensor in practical application, the proposed sensor was applied to the determination of PEA in pig urine samples. No voltammetric response corresponding to PEA was observed when the real samples were analyzed, thus different quantity of PEA was added to the samples. Spiking method was adopted to evaluate the PEA content of different samples. The results were summarized in Table 3. As can be seen from Table 3, the recoveries were from 98.2% to 102.0%. Thus, the RGO-PIL sensor can be used to detect PEA in practical samples with good results.

Table 3. Determination of PEA and recovery test of PEA in pig urine samples with the proposed method (n=5).

Sample	Added PEA (μM)	Found PEA (μM)	Recovery (%)	RSD (%)
Pig urine	0.1	0.0982	98.2	3.8
Pig urine	0.3	0.306	102.0	4.1
Pig urine	0.5	0.496	99.2	4.8

Conclusions

In this paper, an electrochemical sensor based on RGO-PIL has been introduced for PEA determination. The RGO-PIL sensor involved the advantages, such as good electrocatalytic property and large surface area. Due to the synergistic contribution of RGO and PIL, RGO-PIL sensor can be applied for detecting PEA with high sensitivity. Compared with PIL sensor and bare electrode, the RGO-PIL sensor had highest peak current response. Owing to the electrochemical reduction of the nitro group for PEA, 1000-fold of other β-agonists including clenbuterol, ractopamine, and salbutamol did not interfere with PEA determination. The RGO-PIL sensor has been successfully applied to the determination of PEA in pig urine samples. This work may open a new possibility for development of PIL-based materials.

Acknowledgements

This work was supported by the National Natural Science Foundation of China (No. 21177049), the Zhejiang Provincial Natural Science Foundation of China under Grant No. LQ14B050002, the Program for Science and Technology of Jiaxing (No. 2013AY11017) and the University Student Science and Technology Innovation Plan of Zhejiang Province (No. 2014R417007).

Notes and references

[a] *College of Materials Science and Engineering, Changzhou University, Changzhou 213016, P.R. China.*
[b] *College of Biological, Chemical Sciences and Engineering, Jiaxing University, Jiaxing 314001, P.R. China. E-mail: ybzeng@mail.zjxu.edu.cn； lei.li@mail.zjxu.edu.cn.*

1 S. Mehdi Khoshfetrat and M. A. Mehrgardi, *Analyst*, 2014, **139**, 5192-5199.
2 X. Huang, X. Y. Qi, F. Boey and H. Zhang, *Chem. Soc. Rev.*, 2012, **41**, 666-686.
3 C. X. Guo, Z. S. Lu, Y. Lei and C. M. Li, *Electrochem. Commun.*, 2010, **12**, 1237–1240.
4 F. Zhang, Y. Li, Y.-e. Gu, Z. Wang and C. Wang, *Microchim. Acta*, 2011, **173**, 103–109.
5 G. G. Kumar, K. J. Babu, K. S. Nahm and Y. J. Hwang, *RSC Adv.*, 2014, **4**, 7944-7951.
6 A. Afkhami, H. Khoshsafar, H. Bagheri and T. Madrakian, *Anal. Chim. Acta*, 2014, **831**, 50-59.
7 J. H. Zhu, M. J. Chen, Q. L. He, L. Shao, S. Y. Wei and Z. H. Guo, *RSC Adv.*, 2013, **3**, 22790-22824.
8 G. M. Viskadouros, M. M. Stylianakis, E. Kymakis and E. Stratakis, ACS Appl. Mater. Interfaces, 2014, **6**, 388-393.
9 V. Eswaraiah, K. Balasubramaniam and S. Ramaprabhu, Nanoscale, 2012, **4**, 1258-1262.
10 Y. Deng, Y. J. Li, J. Dai, M. D. Lang and X. Y. Huang, J. Poly. Sci. Part A: Polym. Chem., 2011, **49**, 1582-1590.
11 Y. Mao, Y. Bao, S. Y. Gan, F.H. Li and L. Niu, *Biosens. Bioelectron.*, 2011, **28**, 291-297.
12 Y. B. Zeng, Y. Zhou, T. S. Zhou and G. Y. Shi, *Electrochim. Acta*, 2014, **130**, 504-511.
13 H. Liu, K. L. Choy and M. Roe, *Nanoscale*, 2013, **5**, 5725-5731.
14 X. X. Liu, H. Zhu and X. R. Yang, *RSC Adv.*, 2014, **4**, 3706-3712.
15 H. Kim, S. Kobayashi, M. A. AbdurRahim, M. J. Zhang, A. Khusainova, M. A. Hillmyer, A. A. Abdala and C. W. Macosko, *Polymer*, 2011, **52**, 1837-1846.
16 S. Amajjahe and H. Ritter, *Macromol. Rapid Commun.*, 2009, **30**, 94-98.
17 B. Ziolkowski and D. Diamond, *Chem. Commun.*, 2013, **49**, 10308-10310.
18 W. Bi, M. Tian and K. H. Row, *Analyst*, 2012, **137**, 2017-2020.
19 H. Wu, D. Hu, Y. J . Kuang, B. Liu, X. H. Zhang and J. H. Chen, *Angew. Chem. Int. Ed.*, 2009, **121**, 4845-4848.
20 Y. X. Li, G . G. Li, X . W. Wang, Z. Q. Zhu, H. W. Ma, T. Zhang and J. Jin, *Chem. Commun*., 2012, **48**, 8222-8224.
21 X. J. Bo, J. Bai, B. Qi and L. P. Guo, *Biosens. Bioelectron*., 2011, **28**, 77-83.
22 X. Zheng, L. He, Y. Duan, X. Jiang, G. Xiang, W. Zhao and S. Zhang, *J. Chromatogr. A*, 2014, **1358**, 39-45
23 C. M. Tollan, R. Marcilla, J. A. Pomposo, J. Rodriguez, J. Aizpurua, J. Molina and D. Mecerreyes, *ACS Appl. Mater. Interfaces*, 2009, **1**, 348-352.
24 M. N. Li, Y. Z. Liu, S. S. Ding, A. W. Zhu and G. Y. Shi, *Analyst*, 2014, **139**, 5965-5970.
25 Q. Wang and Y. B. Yun, *Microchim. Acta*, 2012, **180**, 261-268.
26 Q. Zhang, S. Y. Wu, L. Zhang, J. Lu, F. Verproot, Y. Liu, Z. Q. Xing, J. H. Li and X. M. Song, *Biosens. Bioelectron.*, 2011, **26**, 2632-2637.
27 X. D. Du, Y. L. Wu, H. J. Yang and T. Yang, *J. Chromatogr. A*, 2012, **1260**, 25-32.
28 E. I. Shishani, S.C. Chai, S. Jamokha, G. Aznar and M.K. Hoffman, *Anal. Chim. Acta*, 2003, **483**, 137-145.
29 X. J. Wang, F. Zhang, F. Ding, W. Q. Li, Q. Y. Chen, X. G. Chu and C. B. Xu, *J. Chromatogr. A*, 2013, **1278**, 82-88.

30 Y. H. Bai , Z. H. Liu , Y. F. Bi, X. Wang, Y. Z. Jin, L. Sun, H. J. Wang, C. M. Zhang and S. X. Xu, *J. Agric. Food Chem.*, 2012, **60**, 11618-11624.

31 M. X. Zhang, C. Li and Y. L. Wu, *J. Chromatogr. B*, 2012, **900**, 94-99.

32 L. L. Zhang, Y. F. Gong, M. Z. Zhang, X. Xi, M. J. Li, Z. L. Chen, X. P. Yu and Y. F. Zhou, *Anal. Methods,* 2014, **6** , 5942-5950.

33 L. J. Cote , F. Kim and J. X. Huang, *J. Am. Chem. Soc.*, 2009, **131**, 1043-1049.

34 O. Akhavan, *Carbon*, 2011, **49**, 11-18.

35 L. Y. Kan, Z. Xu and C. Gao, *Macromolecules*, 2011, **44** , 444-452.

36 N. H. Kim, T. Kuila and J. H. Lee, *J. Hazard. Mater. A*, 2013, **1**, 1349-1358.

37 Y. Liu, L. H. Zhu, Y. Y. Zhang and H. Q. Tang, *Sens. Actuators B*, 2012, **171-172**, 1151-1158.

38 Y. Li, X. Li, C. K. Dong, J. Y. Qi and X. J. Han, Carbon, 2010, **48**, 3427-3433.

39 J. Yan, T. Wei, B. Shao, F. Q. Ma, Z. J. Fan, M. L. Zhang, C. Zheng, Y. C. Shang, W. Z. Qian and F. Wei, *Carbon*, 2010, **48**, 1731-1737.

40 Y. Ouyang, X. Cai, Q. S. Shi, L. L. Liu, D. L. Wan, S. Z. Tan, Y. S. Ouyang, *Colloids Surf. B*, 2013, **107**, 107-114.

41 F. C. Anson, *Anal. Chem.*, 1964, **36**, 932-934.

42 H. S. Yin, Y. L. Zhou, L. Cui, X. G. Liu, S. Y. Ai and L. S. Zhu, *J Solid State Electro.*, 2011, **15**, 167-173.

43 Y. B. Zeng, D. J. Yu and Y. Y. Yu, T. S. Zhou and G. Y. Shi, *J. Hazard. Mater.*, 2012, **217**, 315-322.

44 J. H. Li, D. Z. Kuang, Y. L. Feng, F. X. Zhang, Z. F. Xu and M. Q. Liu, *J. Hazard. Mater.*, 2012, **201-202**, 250-259.

45 A. G. Casado, L. C. Rodriguez, E. A. Hernandez, J. L. Vilchez, *J. Chromatogr. A*, 1996, **726**, 133-139.

46 L. H. Guo, Y. Xu, A. R. Ferhan, G. N. Chen, D. H. Kim, *J. Am. Chem. Soc.*, 2013, **135**, 12338-12345.

47 Y. J. Lai, J. Bai, W. Zhu, Y. Z. Xian and L. T. Jin, *Chin. J. Chem.*, 2013, **31**, 221-229.

48 R. N. Liang, Q. Gao and W. Qin, *Chin. J. Anal. Chem.*, 2012, **40**, 354-358.

49 L. J. Liu, H. B. Pan, M. Du, W. Q. Xie and J. Wang, *Electrochim. Acta*, 2010, **55**, 7240-7245.

50 Y. F. Li, Z. Ye, P. L. Luo, L. Li and B. X. Ye, *Anal. Methods,*2014, **6**, 1928-1935.

51 L. N. Zou, Y. F. Li, S. K. Cao and B. X. Ye, *Electroanalysis*, 2014, **26**, 1051-1058.

52 H. C. Zhang, G. Y. Liu and C. Y. Chai , *Sens. Actuators B*, 2012, **168**, 103-110.

53 X. Yang, B. Feng, P. Yang, Y. L. Ding, Y. Chen and J. J. Fei, *Food Chem.*, 2014, **145**, 619-624.